# Enhancement of Trapped Field and Total Trapped Flux on High Temperature Bulk Superconductor by a New Pulse-Field Magnetization Method



2007 Jpn. J. Appl. Phys. 46 4108

(http://iopscience.iop.org/1347-4065/46/7R/4108)

Japanese Journal of Applied Physics
Vol. 46, No. 7A, 2007, pp. 4108–4112


# Enhancement of Trapped Field and Total Trapped Flux on High Temperature Bulk Superconductor by a New Pulse-Field Magnetization Method

Hiroyuki FUJISHIRO, Tatsuya TATEIWA, and Takuya HIYAMA

*Faculty of Engineering, Iwate University, Morioka 020-8551, Japan*

(Received December 25, 2006; accepted March 19, 2007; published online July 4, 2007)

A higher trapped field $B_T{}^P$ and larger total trapped flux $\Phi_T$ have been achieved on a SmBaCuO bulk superconductor ($\phi$ 45 mm) by a modified multipulse technique with stepwise cooling (MMPSC) and a subsequent iterative magnetizing operation with gradually reduced pulse field amplitude (IMRA). $B_T{}^P = 4.33$ T has been realized at the center of the bulk surface by the MMPSC method, which is higher than that attained by a single-pulse application ($B_T{}^P = 3.3$ T). After the IMRA process, $\Phi_T$ (5 mm) = 1.55 mWb was achieved 5 mm above the bulk surface, which is about 35% larger than that after the MMPSC process. The MMPSC method combined with the IMRA process (MMPSC-IMRA) is demonstrated to be a universal and promising pulse-field magnetization technique for enhancing both $B_T{}^P$ and $\Phi_T$ on any superconducting bulks.
[DOI: 10.1143/JJAP.46.4108]

KEYWORDS: bulk superconductor, pulse-field magnetization, temperature rise, trapped field, MMPSC-IMRA method

## 1. Introduction

As a practical application of REBaCuO bulk superconductors (RE: rare-earth element or yttrium), a high-strength superconducting bulk magnet has been intensively developed by pulse-field magnetization (PFM) as well as the conventional field-cooled magnetization (FCM).[1] The trapped field $B_T{}^P$ obtained by PFM was, however, considerably smaller than that attained by FCM below 77 K due to the large temperature rise ($\Delta T$) caused by the dynamical motion of the magnetic fluxes.[2] Several approaches have been successfully performed to enhance $B_T{}^P$ including an iteratively magnetizing pulsed-field method with reducing amplitude (IMRA)[3] and a multipulse technique with stepwise cooling (MPSC).[4] To clarify the dynamics of the flux motion during PFM and to enhance $B_T{}^P$, we have systematically studied the time and spatial dependences of the temperature $T(t,x)$, local field $B_L(t,x)$, and the trapped field $B_T{}^P$ on the surface of cryocooled REBaCuO bulks during PFM for various starting temperatures $T_s$ and applied fields $B_{ex}$.[5–8] The generated heat $Q$ due to the flux intrusion was estimated using the specific heat $C(T)$ of the bulk and the maximum temperature rise $\Delta T_{max}$. The pinning loss $Q_p$ due to the flux trapping at the pinning centers and the viscous loss $Q_v$ due to the flux movement in the bulk were separately analyzed experimentally and estimated ($Q = Q_p + Q_v$) by successive pulse applications (SPA) with a fixed amplitude.[9] To enhance $B_T{}^P$, both the reduction in $\Delta T$ and the lowering of the bulk temperature $T_s$ are crucial issues, because the critical current density $J_c$ and the resultant trapped field $B_T{}^P$ increase with lowering $T_s$. Taking the obtained experimental results into consideration, we proposed a new PFM technique, which we refer to a modified MPSC (MMPSC), which consists of a two-stage temperature procedure.[10] At the first stage, a small number of magnetic fluxes are trapped at the bulk periphery at a relatively high temperature $T_s(1)$ ($< T_c$; superconducting transition temperature) by the lower-pulse field application of $B_{ex}(1)$. At the second stage, the bulk is cooled to a lower temperature $T_s(2)$ [$< T_s(1)$], and a higher and optimum magnetic pulse field of $B_{ex}(2)$ [$> B_{ex}(1)$] is applied. The temperature rise $\Delta T$ at the second stage can be markedly reduced by the already trapped fluxes at the first stage, compared with that which occurred after the bulk was initially cooled to $T_s(2)$ and the same magnetic field as $B_{ex}(2)$ was applied. We have realized a trapped field of $B_T{}^P = 5.20$ T on a GdBaCuO bulk 45 mm in diameter, which had a trapped field as low as $B_T{}^P = 3.0$ T using a single-pulse application. The value of $B_T{}^P = 5.20$ T is the highest recorded by PFM to date.[11]

In this paper, we apply the MMPSC technique to a REBaCuO bulk disk instead of the GdBaCuO bulk in which $B_T{}^P = 5.20$ T was achieved to demonstrate that the MMPSC method can be universally applied to enhance $B_T{}^P$ for any REBaCuO bulk. The IMRA method is sequentially applied to enhance the total trapped flux $\Phi_T$ after the MMPSC process is complete. The enhancement of $\Phi_T$ as well as that of $B_T{}^P$ is important for applications such as motor and generators using REBaCuO bulks.[12]

## 2. Experimental Methods

A $c$-axis-oriented SmBaCuO bulk superconductor (Dowa Mining) with 45 mm diameter and 18 mm thickness was used. The bulk is composed of $SmBa_2Cu_3O_y$ (Sm123) and $Sm_2BaCuO_5$ (Sm211) with the molar ratio of Sm123 : Sm211 = 1.0 : 0.3, as well as 15.0 wt % $Ag_2O$ powder, and 0.5 wt % Pt powder. A stainless-steel (SUS304) ring with 2.0 mm thickness and 18 mm height was fixed onto the bulk disk using epoxy resin (Stycast 2850GT) to enhance the mechanical strength of the bulk and to reduce the temperature rise due to the increase in heat capacity.[13] Figure 1 shows the experimental setup around the bulk and the pulse coil. The bulk was mounted on a soft iron yoke 40 mm in diameter and 20 mm in thickness and tightly anchored onto the cold stage of a Gifford–McMahon (GM) cycle helium refrigerator. The system was evacuated in the vacuum chamber using an oil diffusion pump. Three Hall sensors (F. W. Bell, model BHT 921) were attached at positions C (bulk center), M (8 mm from the bulk center), and E (16 mm from the bulk center) on the bulk surface. The time evolutions of the local fields [$B_L(C)(t)$, $B_L(M)(t)$, and $B_L(E)(t)$] were monitored using a digital oscilloscope. The bulk was magnetized using a solenoid pulse coil ($L = 1.08$ mH and $R = 0.25\,\Omega$ at 100 K) dipped in liquid $N_2$. The dimensions of the coil are 83 mm in inner diameter, 114 mm in outer diameter, and 112 turns, in which a soft-iron cylinder (40 mm in diameter and 65 mm in thickness) is inserted. The

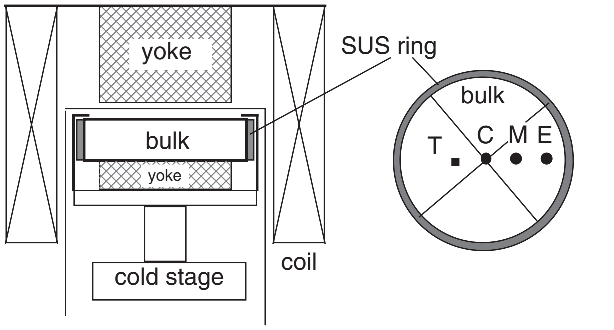


Fig. 1. The experimental setup around the bulk and the pulse coil. The measuring positions of the local field $B_L(t)$ and temperature $T(t)$ are indicated as positions C, M, E, and T on the bulk surface. The trapped field $B_T{}^P$ was measured at position C.

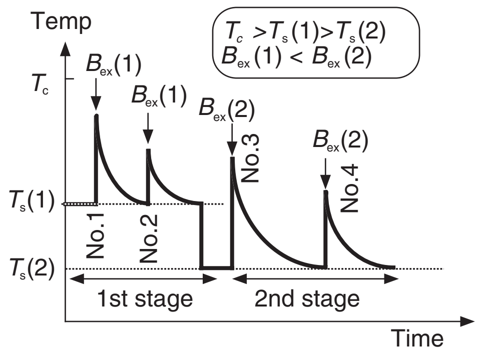


Fig. 2. The concept of the MMPSC technique. The time dependence of the temperature change is schematically shown. Two pulse fields [No. 1 and No. 2; $B_{ex}(1) = 4.0$ T] are applied at the first stage [$T_s(1) = 45$ K] and the higher pulse fields [No. 3 and No. 4; $B_{ex}(2) = 6.0$ T] are subsequently applied at the second stage [$T_s(2) = 30$ K].

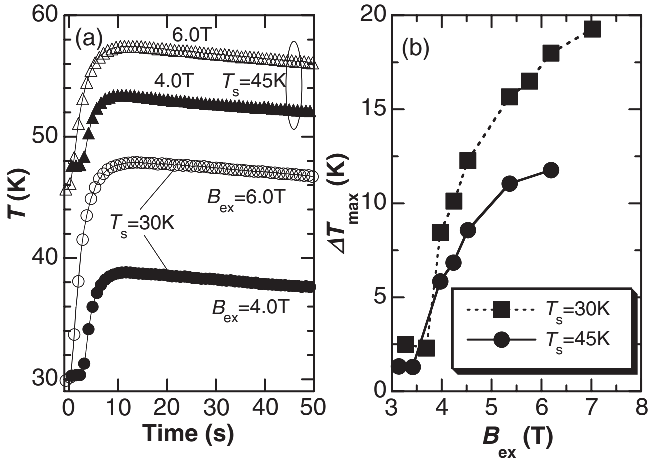


Fig. 3. (a) The time dependences of the temperature $T(t)$ at the position T after a typical magnetic pulse application. (b) The maximum temperature rise $\Delta T_{max}$ as a function of $B_{ex}$ for $T_s = 30$ and 45 K.

applied field $\mu_0 H_a(t)$, of which the maximum strength was defined as $B_{ex}$, was monitored by observing the current $I(t)$ flowing through the shunt resistor. The rising time of the pulse field was 13 ms and the duration was 120 ms. The temperature on the bulk surface $T(t)$ was measured at position T using a fine thermocouple. The total trapped magnetic flux $\Phi_T$ (5 mm) parallel to the $c$-axis of the bulk was measured using an axial Hall sensor, which scanned stepwise on the vacuum chamber 5 mm above the bulk surface with a pitch of 1.2 mm. Figure 2 shows the experimental sequence of the MMPSC technique used in this study. Four magnetic pulses are applied at different initial temperatures, $T_s(1)$ and $T_s(2)$, on the bulk surface. At the first stage, a pulse field $B_{ex}(1) = 4.0$ T was applied twice at $T_s(1) = 45$ K to trap a small number of magnetic fluxes at the bulk periphery. Hereafter, we refer to these two pulses as No. 1 and No. 2. At the second stage, the bulk was cooled to $T_s(2) = 30$ K and a higher pulse field of $B_{ex}(2) = 6.0$ T was applied twice (No. 3 and No. 4). At each stage, the temperature rise $\Delta T$, local fields $B_L(t)$, and the trapped field $B_T{}^P = B_L(C)(t \to \infty)$ were monitored.

## 3. Results and Discussion

### *3.1 Single-pulse application*

To confirm the field-trapping ability of the SmBaCuO bulk used in this study, a single magnetic pulse was applied to the bulk and the trapped field $B_T{}^P$, and temperature rise $\Delta T$ was measured at $T_s = 30$ and 45 K. Figure 3(a) shows the time dependences of the temperature change $T(t)$ at position T for various strengths of the magnetic pulse $B_{ex}$. After applying the pulse field, $T(t)$ rises and takes a maximum at $t \sim 10$ s and then slowly decreases to the initial temperature for $t \sim 15$ min. The temperature rise increases with increasing $B_{ex}$, because a large number of magnetic fluxes intrude into the bulk and destroy the surface potential barrier, and then some of the magnetic fluxes are trapped at the pinning centers. The heat generation results from the pinning loss $Q_p$ and the viscous loss $Q_v$.[9] Figure 3(b) shows the maximum temperature rise $\Delta T_{max}$ as a function of $B_{ex}$ at $T_s = 30$ and 45 K. $\Delta T_{max}$ starts to increase for $B_{ex} > 3.8$ T at $T_s = 30$ K and then increases with increasing $B_{ex}$. On the other hand, at $T_s = 45$ K, $\Delta T_{max}$ starts to increase for $B_{ex} > 3.5$ T and increases less rapidly with increasing $B_{ex}$. These results are mainly due to the enhancement of $Q_p$ at low temperatures. The decrease in the specific heat $C(T)$ of the bulk at low temperatures is another reason.

Figures 4(a) and 4(b) show the trapped field $B_T{}^P$ at position C and the total trapped flux $\Phi_T$ (5 mm) as a function of $B_{ex}$ at $T_s = 30$ and 45 K. In Fig. 4(a), the magnetic fluxes start to intrude and are trapped at the bulk center at $T_s = 30$ K for $B_{ex} > 3.8$ T. $B_T{}^P$ takes a maximum at $B_{ex} = 6.0$ T and then slowly decreases with increasing $B_{ex}$. Note that the $B_T{}^P - B_{ex}$ curve for $T_s = 45$ K shifts parallel to lower $B_{ex}$ by 0.3–0.5 T, compared with that for $T_s = 30$ K. This behavior is closely related with the $\Delta T_{max}$–$B_{ex}$ curve shown in Fig. 3(b), suggesting that the flux movement and trapping result in the generation of heat. The maximum $B_T{}^P$ is equal to almost 3.2 T at $T_s = 30$ and 45 K. In Fig. 4(b), $\Phi_T$ (5 mm) sharply increases for $B_{ex} > 3.8$ T at $T_s = 30$ K and $B_{ex} > 3.5$ T at $T_s = 45$ K, both of which show similar behavior to $B_T{}^P$, as shown in Fig. 4(a). $\Phi_T$ (5 mm) at $T_s = 30$ K is larger than that at $T_s = 45$ K due to the enhancement of the pinning force $F_p$. The $B_{ex}$ values at which the maximum $B_T{}^P$ and maximum $\Phi_T$ (5 mm) can be obtained are slightly different. The maximum values of $B_T{}^P = 3.3$ T and $\Phi_T$ (5 mm) = 1.06 mWb can be obtained at $T_s = 30$ K using the present SmBaCuO bulk by a single-pulse application.

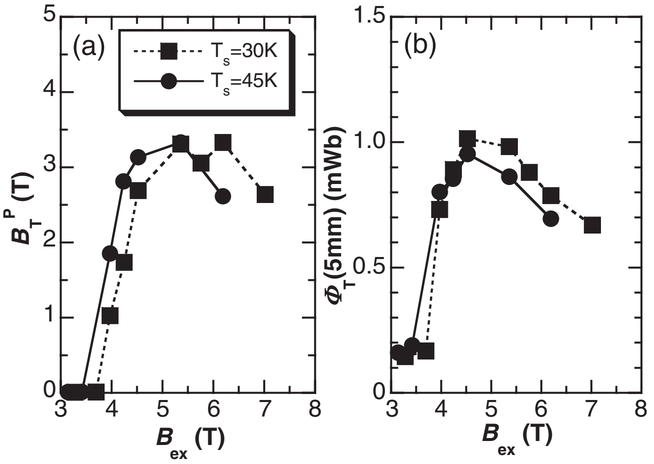


Fig. 4. (a) The trapped field $B_T{}^P$ at the bulk center (position C) and (b) the total trapped flux $\Phi_T$ (5 mm) as a function of the applied pulse field $B_{ex}$ at $T_s = 30$ and 45 K.

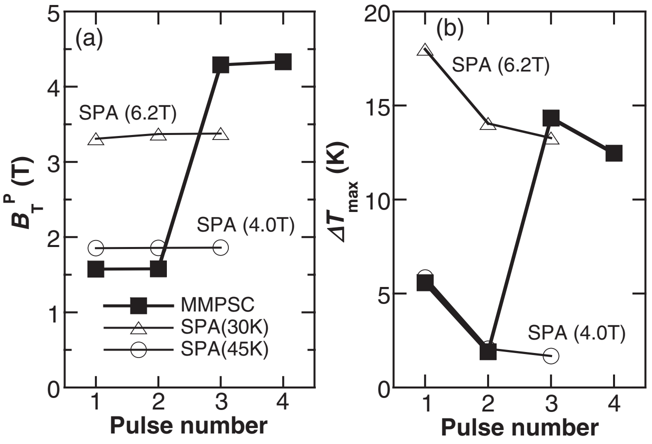


Fig. 6. The pulse-number dependences of (a) the trapped field $B_T{}^P$ and (b) the maximum temperature rise $\Delta T_{max}$ for MMPSC. The results of three pulse applications with the same strength (SPA) are also presented for $B_{ex} = 4.0$ T at $T_s = 45$ K and $B_{ex} = 6.2$ T at $T_s = 30$ K.

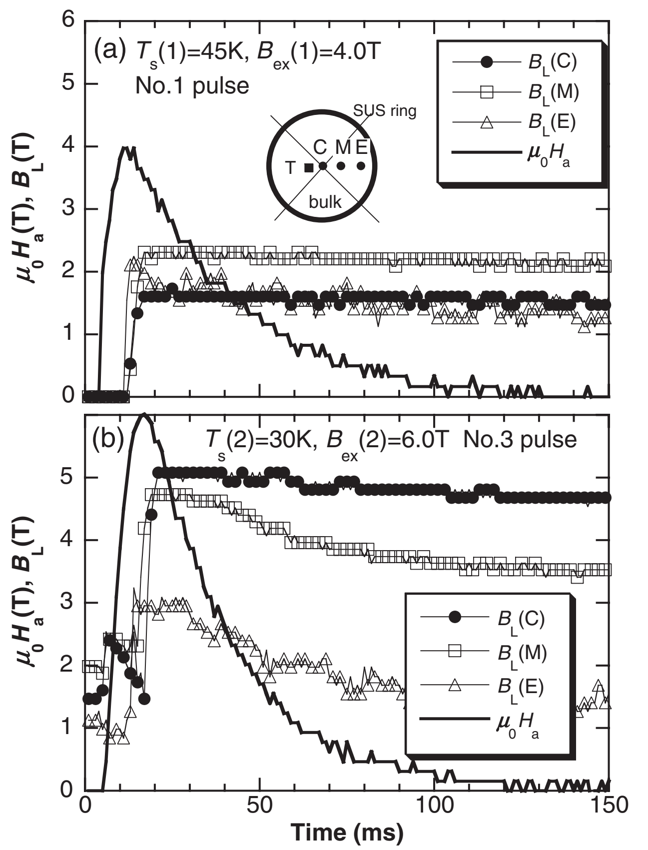


Fig. 5. The time dependences of the applied field $\mu_0 H_a(t)$ and the local fields [$B_L(C)(t)$, $B_L(M)(t)$, $B_L(E)(t)$] after applying (a) pulse No. 1 and (b) pulse No. 3.

### 3.2 MMPSC operation

Taking the experimental results in §3.1 into consideration, the MMPSC process was applied to the SmBaCuO bulk, where $B_{ex}(1) = 4.0$ T was applied twice at $T_s(1) = 45$ K as the first stage and $B_{ex}(2) = 6.0$ T was applied twice at $T_s(2) = 30$ K as the second stage. Figures 5(a) and 5(b) show the time dependences of the applied field $\mu_0 H_a(t)$ and the local fields $B_L(t)$ at positions C, M, and E after applying pulses No. 1 and No. 3, respectively. After applying "pulse No. 1" at the first stage, $B_L(E)(t)$, $B_L(M)(t)$, and $B_L(C)(t)$ sharply increase in this order and quickly reach a final stable value without overshooting. $B_L(M)(t)$ reaches about 2.1 T, but $B_L(C)(t)$ and $B_L(E)(t)$ reach only 1.5–1.3 T. A maximum temperature rise $\Delta T_{max}$ of 5.5 K takes place, which may mainly result from the heat generation due to the flux trapping. For pulse No. 2, $B_T{}^P$ and $B_L(t)$ at C, M, and E remained, and then $\Delta T_{max}$ decreased to 2 K due to a small amount of flux movement. For pulse No. 3 [$B_{ex}(2) = 6.0$ T] at $T_s = 30$ K, as shown in Fig. 5(b), the maximum $B_L(E)(t)$ was only 3 T, which then decreased to 1.2 T, suggesting that the magnetic fluxes inhomogeneously intruded into the bulk from areas other than position E. On the other hand, the maximum of $B_L(C)(t)$ increased to 5.0 T and was as high as 4.6 T after $t = 150$ ms. However, $B_T{}^P = B_T(C)$ gradually decreased to 4.25 T at $t = 15$ min due to the flux creep. $B_L(M)(t)$ increased to 4.7 T then gradually decreased to 3.5 T. After the application of pulse No. 4, $B_T{}^P = B_T(C)$ slightly increased to 4.33 T. When we applied $B_{ex}(2) = 6.2$ T at the second stage, which was slightly higher than $B_{ex}(2) = 6.0$ T, a flux jump occurred and $B_T{}^P$ decreased to 3.8 T. When $B_{ex}(2) = 5.8$ T was applied at the second stage, $B_T{}^P$ reached only 3.6 T. An optimum $B_{ex}(2)$ value exists that enhances the final $B_T{}^P$ value in the MMPSC method.

Figures 6(a) and 6(b) show the pulse-number dependences of the trapped field $B_T{}^P$ and the maximum temperature rise $\Delta T_{max}$ for the present MMPSC method, respectively. For comparison, the results for three successive magnetic pulse applications (SPA) with the same strength are also shown for $B_{ex} = 4.0$ T at $T_s = 45$ K, which correspond to the conditions at the first stage, and for $B_{ex} = 6.2$ T at $T_s = 30$ K, which nearly corresponds to the conditions at the second stage. In the SPA process at $T_s = 30$ K, a field of $B_T{}^P = 3.20$ T was trapped after the pulse No. 1, and the trapped field increased very slightly to 3.35 T after the No. 3 pulse. $\Delta T_{max}$ gradually decreased from 18 K after the pulse No. 1 to 13 K after pulse No. 3. Similar pulse-number dependences of $B_T{}^P$ and $\Delta T_{max}$ were also shown after SPA for $B_{ex} = 4.0$ T at $T_s = 45$ K. For the first stage (No. 1 and No. 2 pulses) in the MMPSC process, $B_T{}^P$ and $\Delta T_{max}$ have similar traces to those after SPA. However, the $B_T{}^P$ value after pulse No. 3 jumps to $B_T^P = 4.25$ T then slightly increases to 4.33 T after pulse No. 4. Note that $\Delta T_{max}$ is 14.5 K after pulse No. 3 in MMPSC, which is about 4 K lower than that after pulse No. 1 in SPA. The reduction in $\Delta T_{max}$ is due to the already trapped fluxes at the first stage, which enhance the $B_T^P$ value in the MMPSC process. In the previous paper, we suggested that, at the first stage, the field trapping ($B_T^P \sim 1$ T) into the bulk center, which has an *M-shaped* trapped-field distribution, should critically govern the final $B_T^P$ value.[14] The *M-shaped* distribution means that the trapped field at position C is lower than that at position M and/or position E. In the present MMPSC, the desirable *M-shaped* profile [$B_T^P = B_T(C) = 1.5$ T, $B_T(M) = 2.1$ T] was realized at the first stage. The optimization of $T_s$ and $B_{ex}$ for each stage is of crucial importance for attaining a $B_T^P$ value higher than 4 T. Since the SPA technique is also effective in reducing the temperature rise, it is necessary to apply the same $B_{ex}$ twice for each stage.

### *3.3 Enhancement of $\Phi_T$ by subsequent IMRA method*

After the termination of the MMPSC process for pulse No. 4, the IMRA method was applied to enhance the $\Phi_T$ value. In the IMRA method, several magnetizing pulsed fields with reduced amplitude are iteratively applied to the bulk at constant $T_s$ and the additional fluxes are trapped around the bulk periphery. As a result, the total trapped flux $\Phi_T$ increases.[3] Figure 7 shows the pulse-number dependence of the total trapped flux $\Phi_T$ (5 mm) during the MMPSC and IMRA processes. The results of the trapped field $B_T^P$ are also shown. The pulse numbers from No. 5 to No. 14 correspond to the IMRA process, which was performed at $T_s = 30$ K. The inset shows the relation between $\Phi_T$ (5 mm) and $B_{ex}$ for each pulse in the MMPSC-IMRA process. $\Phi_T$ (5 mm) increases with increasing magnetic pulse number; $\Phi_T$ (5 mm) is 1.15 mWb for No. 5 and is 1.55 mWb for No. 14, which is an increase of 35% during the IMRA process. On the other hand, $B_T^P$ on the bulk surface is not enhanced during the IMRA process.

Figure 8 shows the cross sections of the trapped field profile $B_T$ (5 mm) on the surface of the vacuum chamber, which is 5 mm above the bulk surface for different pulse numbers. The trapped-field profile shows a symmetric cone-shaped distribution. The change in the profile from pulse No. 2 to pulse No. 4 results from the trapped-field enhancement due to the MMPSC method. The $B_T$ (5 mm) value increases from 1.4 to 1.7 T after the 10 pulses in the IMRA method. The enhancement in $B_T$ (5 mm) is not due to the trapped field enhancement at the center of the bulk surface but due to the additional flux trapping at the bulk periphery.

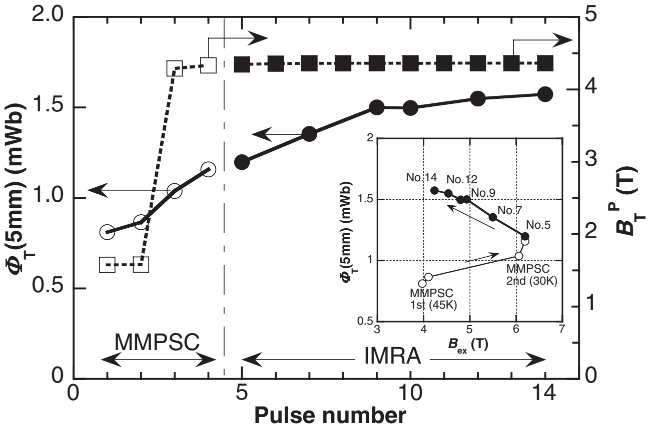


Fig. 7. The pulse-number dependence of the total trapped flux $\Phi_T$ (5 mm) and the trapped field $B_T^P$ for the MMPSC-IMRA method. The inset shows $\Phi_T$ (5 mm) as a function of applied field $B_{ex}$.

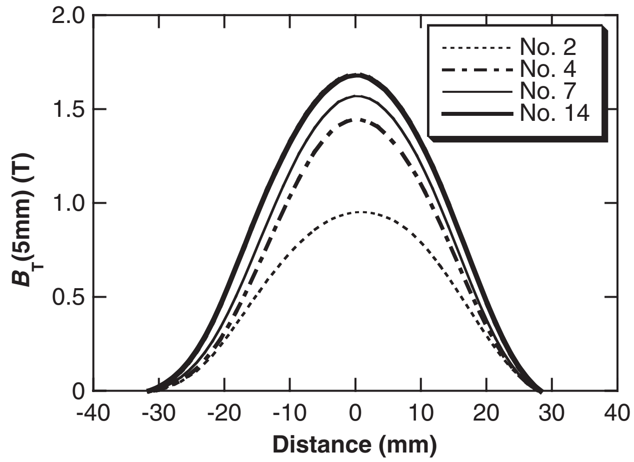


Fig. 8. The trapped-field profiles $B_T$ (5 mm) 5 mm above the bulk surface in air for the MMPSC process (No. 2 and No. 4) and for the IMRA process (No. 7 and No. 14).

## 4. Conclusions

A higher trapped field $B_T^P$ and a larger total trapped flux $\Phi_T$ have been achieved on a SmBaCuO bulk superconductor by a modified multipulse technique with stepwise cooling (MMPSC) and a subsequent iterative magnetizing operation with gradually reduced pulse field amplitude (IMRA). $B_T^P = 4.33$ T has been realized on the bulk surface by the MMPSC method, which is higher than that attained by the single-pulse technique ($B_T^P = 3.3$ T). After additional 10 pulses in the IMRA method, $\Phi_T$ (5 mm) = 1.55 mWb was achieved 5 mm above the bulk surface, which is about 35% larger than that after the MMPSC process. The generated magnetic field $B_T$ (5 mm), 5 mm above the bulk surface in air is 1.7 T after the IMRA process, which is about 21% larger than that before the IMRA process. Thus, the MMPSC method is demonstrated to be a universal and promising PFM technique for enhancing both $B_T^P$ for any REBaCuO bulk, and the subsequent IMRA technique can be used to enhance the $\Phi_T$ and $B_T$ values in air.


## Acknowledgments

The authors thank Professor T. Oka of Niigata University for the valuable discussions. This work is supported in part by a Grant-in-Aid for Scientific Research from the Ministry of Education, Culture, Sports, Science and Technology, Japan (No. 17560001) and from Iwate Prefecture, Japan.



1) U. Mizutani, H. Hazama, T. Matsuda, Y. Yanagi, Y. Itoh, K. Sakurai, and A. Imai: Supercond. Sci. Technol. **16** (2003) 1207.
2) H. Ishihara, H. Ikuta, Y. Itoh, Y. Yanagi, M. Yoshikawa, T. Oka, and U. Mizutani: Physica C **357–360** (2001) 763.
3) U. Mizutani, T. Oka, Y. Itoh, Y. Yanagi, M. Yoshikawa, and H. Ikuta: Appl. Supercond. **6** (1998) 235.
4) M. Sander, U. Sutter, R. Koch, and M. Klaser: Supercond. Sci.

Technol. **13** (2000) 841.
5) H. Fujishiro, T. Oka, K. Yokoyama, and K. Noto: Supercond. Sci. Technol. **16** (2003) 809.
6) H. Fujishiro, K. Yokoyama, T. Oka, and K. Noto: Supercond. Sci. Technol. **17** (2004) 51.
7) H. Fujishiro, K. Yokoyama, M. Kaneyama, M. Ikebe, T. Oka, and K. Noto: Physica C **426–431** (2005) 594.
8) H. Fujishiro and S. Kohayashi: IEEE Trans. Appl. Supercond. **12** (2002) 1124.
9) H. Fujishiro, K. Yokoyama, M. Kaneyama, T. Oka, and K. Noto: Physica C **412–414** (2004) 646.
10) H. Fujishiro, M. Kaneyama, T. Tateiwa, and T. Oka: Jpn. J. Appl. Phys. **44** (2005) L1221.
11) H. Fujishiro, T. Tateiwa, A. Fujiwara, T. Oka, and H. Hayashi: Physica C **445–448** (2006) 334.
12) M. Miki, S. Tokura, H. Hayakawa, H. Inami, M. Kitano, H. Matsuzaki, Y. Kimura, I. Ohtani, E. Morita, H. Ogata, M. Izumi, H. Sugimoto, and T. Ida: Supercond. Sci. Technol. **19** (2006) S494.
13) H. Fujishiro, K. Yokoyama, M. Kaneyama, T. Oka, and K. Noto: IEEE Trans. Appl. Supercond. **15** (2005) 3762.
14) H. Fujishiro, M. Kaneyama, T. Tateiwa, and T. Oka: J. Phys.: Conf. Ser. **43** (2006) 405.